

Thermal Analysis of Effect of a Compartment Fire on Window Glass

A. Joshi[†] and P. J. Pagni[‡]

Department of Mechanical Engineering
University of California
Berkeley, CA 94720, USA

[†] Graduate Student
[‡] Professor

ABSTRACT

Glass breaking in fires is an important practical problem since a window acts as a wall prior to breaking and as a vent after breaking. This geometric change can have a dramatic effect on the evolution of a compartment fire. As Emmons explained, windows break in fires due to thermal stress from the differential heating of the central portion and the shaded edge. If the depth of shading around the edge is much greater than the glass thickness, one can assume that the edge remains at its initial temperature T_i . This paper determines the surface temperature history, $T'(0,t')$, of the glass. The temperature at breaking is when $(T'(0,t') - T_i)\alpha = \sigma_b/E$, where $\alpha\Delta T$ and σ_b/E both give the strain at breaking in tension. The glass coefficient of linear thermal expansion is α , the glass modulus is E and σ_b is its tensile strength. Typical property values suggest the range $50^\circ\text{C} - 100^\circ\text{C}$ for the breaking ΔT . Here the transient, one-dimensional (into the glass normal to the pane), in-homogeneous (in-depth radiation absorption) energy equation is solved using an innovative Laplace Transform technique suggested by Baum. Two coupled non-linear Volterra equations of the second kind are obtained for the temperatures of the two surfaces of the glass. Time varying incident radiative flux and the glass temperatures are included. These equations are solved numerically by using the trapezoidal rule for numerical integration and Newton-Raphson's method for determining the roots of the non-linear equations. Results are presented for typical values of the governing dimensionless parameters.

INTRODUCTION

Breaking of window glass due to heat from fires is a very commonly observed phenomenon. This phenomenon is of great importance as the glass breakage can be a cause of fire spread (if the window is between two adjoining rooms) or a broken window can act as a vent for the escape of toxic fire gases and an inlet for fresh air (if the window opens to the outside). Glass absorbs thermal radiation from the fire and also gets heated by convection from the hot air surrounding the fire leading to thermal stresses. The thermal stresses arise due to the temperature difference between the central portion of the window which is exposed to fire products and the insulated or protected edge of the window. These stresses lead to cracks and eventually to breakage. In this paper, a thermal analysis of the effect of radiation and convection on the glass is carried out by including the exponential decay of thermal radiation within the glass and heating and/or cooling of the surfaces due to convection and radiation heat transfer.

Emmons (1986) indicated that the process of the initiation and propagation of cracks in glass due to the heat is not very well understood. Finnie et al (1985) carried out an analysis which implied that the only factor governing the breakage is the net temperature difference between the central heated portion of the glass and the protected edge, which can be calculated from the glass properties. Since the protected edge temperature is not expected to rise much in a fire, the difference between the temperature of the central portion and the edge can be approximated by the net temperature rise of the heated portion. The side exposed to the fire is expected to have the highest temperature and thus a knowledge of the temperature history of only this side is adequate in determining the time for breakage.

The problem governing this phenomenon is transient and non-linear due to the radiation boundary condition. Keski-Rahkonen (1988) linearized the boundary conditions and obtained an exact solution for the temperature field. Recently, Davies (1985) used an integral method for determining the temperature field in a plate losing heat by combined radiation and convection. In Davies' method, inaccuracies arise due to the assumed nature of the temperature profile. For solving the complete non-linear problems the use of a numerical method is essential. Methods such as finite-difference, finite-element and boundary element have been used before. However the implementation of these methods leads to

the inaccuracies arising from the discretization of both the time and space domain. Also the whole temperature field has to be evaluated. In the present case, the temperature of interest is only of the side exposed to the fire and hence the knowledge of the whole temperature field is irrelevant.

The thickness of the window is usually an order of magnitude smaller than the other dimensions and so in the case discussed, the window has been assumed to be an infinite slab. Thus the equation governing the system is a one dimensional inhomogeneous heat equation with non-linear boundary conditions. To solve this equation, the method of Laplace transform is utilized. After simplifications, only two equations for the temperature of each surface need to be solved. This method is similar to Chambres (1959) method which was used to determine the temperature distribution in a semi-infinite solid with radiation type boundary conditions. In Chambres methods one non-linear Volterra equation of the second kind for the surface temperature needs to be solved, whereas in the present case, a system of two coupled non-linear Volterra equations of the second kind for the temperatures of each side have to be solved. These equations are solved numerically by using the trapezoidal rule for numerical integration and Newton-Raphson's method for determining the roots of the non-linear equations. The equations are exact and inaccuracies arise only due to the discretization of the time domain. This method is applied to the general case of time varying radiative flux and surrounding temperatures.

THEORY AND FORMULATION

Consider an infinite slab of thickness L , initially at a temperature T_i . At time $t' = 0$ it starts getting heated on the side $x = 0$ due to radiative flux $I_{\alpha} j'(t')$ and loses or gains heat by combined convection and radiation on both sides. Suppose the heat transfer coefficients on the two sides are represented by h_1 and h_2 , the ambient temperatures are represented by $T_{1\infty}(t')$ and $T_{2\infty}(t')$. Let β be the absorption length and k be the thermal conductivity of glass. Also let ρ and C_p be the density and specific heat respectively of the glass. Also let ϵ and ϵ_{∞} be the emissivities of the glass and the surroundings. σ is the Stefan-Boltzmann constant. Then the governing equation for this system will be

$$\rho C_p \frac{\partial T'}{\partial t'} = k \frac{\partial^2 T'}{\partial x'^2} + I_{\alpha} j'(t') \frac{e^{-x' \cdot \beta}}{\beta} \quad (1)$$

where $f'(t')$ is some specified function of time. The initial and boundary conditions for this problem are

$$\text{at } t' = 0, T' = T_i \quad (2)$$

$$\text{at } x' = 0, -k \frac{\partial T'}{\partial x'} = h_2(T_{2\infty}(t') - T'(0, t')) - \epsilon \sigma T'^4(0, t') \quad (3)$$

$$\text{at } x' = L, -k \frac{\partial T'}{\partial x'} = h_1(T'(L, t') - T_{1\infty}(t)) + \epsilon \sigma T'^4(L, t') - \epsilon_\infty \sigma T_{1\infty}^4(t) \quad (4)$$

Nondimensionalization

This equation is nondimensionalized by using the following dimensionless variables

$$x = \frac{x'}{L}; t = \frac{t' k}{\rho C_p L^2}; T = \frac{T' - T_i}{T_c}; \gamma = \frac{\beta}{L} \quad (5)$$

where T_c is the characteristic temperature defined by

$$T_c = \frac{l_o L}{k} \quad (6)$$

Hence, in the dimensionless form, the governing equation becomes

$$\frac{\partial T}{\partial t} = \frac{\partial^2 T}{\partial x^2} + j(t) \frac{e^{-x/\gamma}}{\gamma} \quad (7)$$

with initial and boundary conditions

$$\text{at } t = 0, T = 0 \quad (8)$$

$$\text{at } x = 0, -\frac{\partial T}{\partial x} = q_2(t) \quad (9)$$

$$\text{at } x = 1, -\frac{\partial T}{\partial x} = q_1(t) \quad (10)$$

where

$$q_2(t) = A + BT(0, t) + CT^2(0, t) + DT^3(0, t) + ET^4(0, t) \quad (11)$$

and

$$q_1(t) = F + GT(1,t) - CT^2(1,t) - DT^3(1,t) - ET^4(1,t) \quad (12)$$

where

$$A = \frac{h_2L(T_{2\infty}(t)-T_i)}{kT_c} - \frac{\epsilon\sigma LT_i^4}{kT_c} \quad (13)$$

$$B = -\frac{h_2L}{k} + \frac{4\epsilon\sigma T_i^3L}{k} \quad (14)$$

$$C = -\frac{6\epsilon\sigma T_c T_i^2L}{k} \quad (15)$$

$$D = -\frac{4\epsilon\sigma T_c^2 T_i L}{k} \quad (16)$$

$$E = -\frac{\epsilon\sigma T_c^3 L}{k} \quad (17)$$

$$F = \frac{h_1L(T_i-T_{1\infty})}{kT_c} - \frac{\epsilon_{\infty}\sigma T_{1\infty}^4L}{kT_c} + \frac{\epsilon\sigma LT_i^4}{kT_c} \quad (18)$$

$$G = \frac{h_1L}{k} + \frac{4\epsilon\sigma T_i^3L}{k} \quad (19)$$

METHOD OF SOLUTION

We use the method of Laplace transforms to solve this equation. The Laplace transform is taken with respect to time and is defined as

$$T^* = \int_0^{\infty} T e^{-pt} dt \quad (20)$$

Substituting the transformed variable into the governing equation and applying the boundary conditions leads to the solution

$$T^* = A_1 j^* \frac{e^{-x/\gamma}}{\gamma} + B_1 \cosh(\sqrt{p}x) + C_1 \cosh(\sqrt{p}(1-x)) \quad (21)$$

where

$$A_1 = \frac{1}{p - \frac{1}{\gamma^2}} \quad (22)$$

$$B_1 = \frac{A_1 j^* e^{-1/\gamma} - \gamma^2 q_1^*}{\gamma^2 \sqrt{p} \sinh \sqrt{p}} \quad (23)$$

$$C_1 = \frac{\gamma^2 q_2^* - A_1 j^*}{\gamma^2 \sqrt{p} \sinh \sqrt{p}} \quad (24)$$

We need to solve for both the surface temperatures as the temperature on the hotter surface depends on the temperature on the other surface and vice versa. Hence, the transformed form of the temperatures are

$$T^*(0) = \frac{A_1 j^*}{\gamma} + B_1 + C_1 \cosh \sqrt{p} = f_1^* q_1^* + f_2^* q_2^* + \frac{1}{\gamma} f_3^* j^* \quad (25)$$

$$T^*(1) = \frac{A_1 e^{-1/\gamma} j^*}{\gamma} + B_1 \cosh \sqrt{p} + C_1 = g_1^* q_1^* + g_2^* q_2^* + \frac{1}{\gamma} g_3^* j^* \quad (26)$$

Using convolution theorem and after simplifications, the equations to be solved look like

$$T(0,t) = \int_0^t q_1(\tau) f_1(t-\tau) d\tau + \int_0^t q_2(\tau) f_2(t-\tau) d\tau + \frac{1}{\gamma} \int_0^t j(\tau) f_3(t-\tau) d\tau \quad (27)$$

and

$$T(1,t) = \int_0^t q_1(\tau) g_1(t-\tau) d\tau + \int_0^t q_2(\tau) g_2(t-\tau) d\tau + \frac{1}{\gamma} \int_0^t j(\tau) g_3(t-\tau) d\tau \quad (28)$$

where $f_1, f_2, f_3, g_1, g_2, g_3$ are the kernels which depend upon γ and are specified in Appendix I. The equations to be solved are coupled non-linear Volterra equations of the second kind. The equations are non-linear because both q_1 and q_2 are non-linear functions of T_1 and T_2 respectively.

Transformation of variable

We observe that the integrands are not bounded as $f_2(t)$ and $g_1(t)$ at $t = 0$ go to infinity as $t^{-1/2}$. So if we now transform the equations using the variable $u = \sqrt{t-\tau}$, the equations become

$$T(0,t) = 2 \int_0^{\sqrt{t}} u F_1(u) q_1(t-u^2) du + 2 \int_0^{\sqrt{t}} u F_2(u) q_2(t-u^2) du + \frac{2}{\gamma} \int_0^{\sqrt{t}} u F_3(u) j(t-u^2) du \quad (29)$$

and

$$T(1,t) = 2 \int_0^{\sqrt{t}} u G_1(u) q_1(t-u^2) du + 2 \int_0^{\sqrt{t}} u G_2(u) q_2(t-u^2) du + \frac{2}{\gamma} \int_0^{\sqrt{t}} u G_3(u) j(t-u^2) du \quad (30)$$

where $F_1(u) = f_1(u^2)$ etc. and the integrands are bounded.

Numerical procedure

The numerical procedure chosen was trapezoidal rule with constant time steps (thus variable Δu) for numerical integration and Newton-Raphson's methods for finding roots of the non-linear equations. By looking at the equations, it appears that the equations are coupled. However, since $f_1(0)$ and $g_2(0)$ are equal to 0, at a particular time step the equations can be solved independently of one another.

RESULTS

Figure 1 shows the comparison with the exact solution of the linear problem (given in Appendix II) for the case of no heat loss due to thermal radiation. This figure shows the dimensionless temperature variation with respect to dimensionless time of the sides exposed and unexposed to incoming radiative flux. The agreement is within 0.5% for a dimensionless time step of 0.002 suggesting that the the time step was quite accurate.

Figures 2(a) and (b) show respectively the variation with respect to time of the dimensionless temperature of the side exposed to and the side unexposed to the incoming heat flux. Only the Biot numbers were changed. In this case the initial temperature of the material is set equal to the ambient temperatures on either sides. Also the incoming radiative flux is assumed to have a constant value. The ambient temperatures are assumed to be constant.

As expected, the temperature of the side exposed to the heat flux increases more rapidly compared to the temperature of the unexposed side. As Biot numbers increase, heat loss is greater and hence the rate of increase of temperature is lower.

Figure 3 shows the variation of the temperatures for varying dimensionless absorption length for constant value of Biot number. Here also, the input radiative flux function is assumed to be a

constant. Here, as γ decreases, the temperature of the exposed side increases as small γ corresponds to small absorption length, implying that most of the radiation gets absorbed within a short distance. And for large values of γ , the material behaves more like a transparent medium. For large values of γ an artificial temperature drop is encountered as the approximation of surface emission but absorption within the body breaks down.

Figure 4 shows the variation of the temperatures of the sides corresponding to varying input radiation flux, holding the other parameters constant. It can be seen here that the rate of increase of the temperature of the exposed side varies roughly as the integral with respect to time of the incoming radiation function. This is because the rate of increase of temperature is dependent on the rate of incoming heat as can be seen in equation (29) for $T(0,t)$.

Table 1 shows the various values used for the calculations. These values represent the typical values which might be encountered in the situations of real fires. The time of glass breakage solely depends upon the net temperature rise of the glass, and it was found that for ordinary plate glass, the value was found to be about 60° C. This value is obtained from Hooke's law and it was verified by Finnie et. al. that this value does not depend on the rate of temperature rise. This would imply that for a particular value of the radiative flux, a value of the dimensionless critical temperature can be obtained. Hence in the computer program, the computations are stopped as soon as the critical temperature is reached.

REFERENCES

- Chambres, P. L. (1959) "Nonlinear Heat Transfer Problem", *Journal of Applied Physics*, vol.30, no.11, pp 1683-1688.
- Davies, T. W. (1985) "The Cooling of a Plate by Combined Thermal Radiation and Convection", *International Communication in Heat and Mass Transfer*, vol.12, pp 405-415.
- Emmons, H. W. (1986) "The Needed Fire Science", *First International Symposium on Fire Safety Science*, pp 33-53.

Finnie, I and Chang, Wei-Li (1985) *private communication*.

Keski-Rahkonen, Olavi (1988) "Breaking of Window Glass Close to Fire". *Fire and Materials*, vol.12, pp 61-69.

APPENDIX I

The Laplace transforms of the kernels in equations are

$$f_1^* = \frac{-1}{\sqrt{p} \sinh(\sqrt{p})} \quad (31)$$

$$f_2^* = \frac{\cosh(\sqrt{p})}{\sqrt{p} \sinh(\sqrt{p})} \quad (32)$$

$$g_1^* = -f_2^* \quad (33)$$

$$g_2^* = -f_1^* \quad (34)$$

$$f_3^* = \frac{\gamma\sqrt{p} \sinh(\sqrt{p}) + e^{-1/\gamma} - \cosh(\sqrt{p})}{(p - \frac{1}{\gamma^2})\gamma\sqrt{p} \sinh(\sqrt{p})} \quad (35)$$

$$g_3^* = \frac{\gamma\sqrt{p} \sinh(\sqrt{p})e^{-1/\gamma} + \cosh(\sqrt{p})e^{-1/\gamma} - 1}{(p - \frac{1}{\gamma^2})\gamma\sqrt{p} \sinh(\sqrt{p})} \quad (36)$$

And hence the kernels are

for short time

$$f_1(t) = -g_2(t) = -\frac{2}{\sqrt{\pi t}} \sum_{k=0}^{\infty} \exp\left[-\frac{(2k+1)^2}{4t}\right] \quad (37)$$

$$f_2(t) = -g_1(t) = \frac{1}{\sqrt{\pi t}} + \frac{2}{\sqrt{\pi t}} \sum_{k=1}^{\infty} \exp\left[-\frac{(2k)^2}{4t}\right] \quad (38)$$

$$f_3(t) = e^{\frac{1}{\gamma^2}} \left\{ 1 + \right.$$

$$\begin{aligned}
& e^{-1/\gamma} \sum_{k=0}^{\infty} \left[e^{-\frac{2k+1}{\gamma}} \operatorname{erfc} \left[\frac{(2k+1)}{\sqrt{4t}} - \frac{\sqrt{t}}{\gamma} \right] - e^{\frac{2k+1}{\gamma}} \operatorname{erfc} \left[\frac{(2k+1)}{\sqrt{4t}} + \frac{\sqrt{t}}{\gamma} \right] \right] \\
& - \frac{1}{2} \left[\operatorname{erfc} \left(-\frac{\sqrt{t}}{\gamma} \right) - \operatorname{erfc} \left(\frac{\sqrt{t}}{\gamma} \right) \right] \\
& - \sum_{k=1}^{\infty} \left[e^{-\frac{2k}{\gamma}} \operatorname{erfc} \left[\frac{2k}{\sqrt{4t}} - \frac{\sqrt{t}}{\gamma} \right] - e^{\frac{2k}{\gamma}} \operatorname{erfc} \left[\frac{2k}{\sqrt{4t}} + \frac{\sqrt{t}}{\gamma} \right] \right] \quad (39)
\end{aligned}$$

$$\begin{aligned}
g_3(t) &= e^{\frac{t}{\gamma^2}} \left\{ e^{-1/\gamma} - \right. \\
& \sum_{k=0}^{\infty} \left[e^{-\frac{2k+1}{\gamma}} \operatorname{erfc} \left[\frac{(2k+1)}{\sqrt{4t}} - \frac{\sqrt{t}}{\gamma} \right] - e^{\frac{2k+1}{\gamma}} \operatorname{erfc} \left[\frac{(2k+1)}{\sqrt{4t}} + \frac{\sqrt{t}}{\gamma} \right] \right] \\
& + \frac{e^{-1/\gamma}}{2} \left[\operatorname{erfc} \left(-\frac{\sqrt{t}}{\gamma} \right) - \operatorname{erfc} \left(\frac{\sqrt{t}}{\gamma} \right) \right] \\
& \left. + e^{-1/\gamma} \sum_{k=1}^{\infty} \left[e^{-\frac{2k}{\gamma}} \operatorname{erfc} \left[\frac{2k}{\sqrt{4t}} - \frac{\sqrt{t}}{\gamma} \right] - e^{\frac{2k}{\gamma}} \operatorname{erfc} \left[\frac{2k}{\sqrt{4t}} + \frac{\sqrt{t}}{\gamma} \right] \right] \right\} \quad (40)
\end{aligned}$$

and for long time are

$$f_1(t) = -g_2(t) = - \left[1 + 2 \sum_{k=1}^{\infty} e^{-k^2 \pi^2 t} (-1)^k \right] \quad (41)$$

$$f_2(t) = -g_1(t) = 1 + 2 \sum_{k=1}^{\infty} e^{-k^2 \pi^2 t} \quad (42)$$

$$f_3(t) = -\gamma(e^{-1/\gamma} - 1) + \frac{2}{\gamma} \sum_{k=1}^{\infty} \frac{(-1)^k e^{-1/\gamma} - 1}{-k^2 \pi^2 - \frac{1}{\gamma^2}} e^{-k^2 \pi^2 t} \quad (43)$$

$$g_3(t) = -\gamma(e^{-1/\gamma} - 1) + \frac{2}{\gamma} \sum_{k=1}^{\infty} \frac{e^{-1/\gamma} - (-1)^k}{-k^2 \pi^2 - \frac{1}{\gamma^2}} e^{-k^2 \pi^2 t} \quad (44)$$

APPENDIX II

The exact solution to the linear problem of negligible heat loss due to radiation is

$$T = u(x,t) + v(x) \quad (45)$$

where

$$v(x) = \rho x + q \quad (46)$$

where

$$\rho = -\frac{ABi_1 + BBi_2}{Bi_1 + Bi_2 + Bi_1Bi_2} \text{ and } q = -\frac{B - A - ABi_1}{Bi_1 + Bi_2 + Bi_1Bi_2} \quad (47)$$

Here

$$A = \frac{T_{2\infty} - T_i}{T_c} Bi_2, \quad B = \frac{T_i - T_{1\infty}}{T_c} Bi_1 \quad (48)$$

where

$$Bi_1 = \frac{h_1 L}{k} \text{ and } Bi_2 = \frac{h_2 L}{k} \quad (49)$$

where h_1 and h_2 are the heat transfer coefficients. The solution for $u(x,t)$ is given by

$$u = \sum_{n=0}^{\infty} \left[C_n e^{-\lambda_n^2 t} + \int_0^t e^{-\lambda_n^2(t-\tau)} w_n(\tau) d\tau \right] \phi_n(x) \quad (50)$$

where the characteristic functions are

$$\phi_n(x) = \lambda_n \cos(\lambda_n x) + Bi_2 \sin(\lambda_n x) \quad (51)$$

and the eigenvalues λ_n are obtained from the solutions to

$$\cot \lambda_n = \frac{\lambda_n^2 - Bi_1 Bi_2}{\lambda_n (Bi_1 + Bi_2)} \quad (52)$$

The constants C_n appearing in the equation for $u(x,t)$ are defined as

$$C_n = -\frac{1}{N(\lambda_n)} \int_0^1 v(x) \phi_n(x) dx \quad (53)$$

the weight functions w_n are defined as

$$w_n(t) = \frac{1}{\gamma N(\lambda_n)} \int_0^1 j(t) e^{-x/\gamma} \phi_n(x) dx \quad (54)$$

and norms $N(\lambda_n)$ are defined as

$$N(\lambda_n) = \frac{1}{2} \left[(\lambda_n^2 + Bi_2^2) \left(1 + \frac{Bi_1}{\lambda_n^2 + Bi_1^2} \right) + Bi_2 \right] \quad (55)$$

Table 1. Glass and Fire Parameters

thermal conductivity,	$k = 0.76 W/mK$
thermal diffusivity,	$\alpha = 3.6 \times 10^{-7} m^2/s$
thickness,	$L = 6.25 \times 10^{-3} m$
penetration depth,	$\beta = 10^{-3} m, 3.13 \times 10^{-3} m, 6.25 \times 10^{-4} m$
temperatures,	$T_{1\infty} = T_{2\infty} = T_i = 293 K$
emissivities,	$\varepsilon = 1.0, \varepsilon_{\infty} = 1.0$
incident flux,	$I_0 = 1000 W/m^2K$

FIGURE CAPTIONS

Figure 1. The surface temperatures, $T(0,t)$ and $T(1,t)$ are shown where $T = (T' - T_1)k/h_0L$ and $t = t' \alpha/L^2$ for $\gamma = 0.16$ and $Bi_1 = Bi_2 = 0.1$. The exact linearized results and numerical results are indistinguishable.

Figure 2. The variation of the exposed surface temperature with Biot number for $Bi = Bi_1 = Bi_2$ is shown for $\gamma = 0.16$ and the other parameters as listed in Table 1.

Figure 2. The variation of the unexposed surface temperature with Biot number for $Bi = Bi_1 = Bi_2$ is shown for $\gamma = 0.16$ and the other parameters as listed in Table 1.

Figure 3. The variation of the exposed surface temperature with depth parameter, γ , for $Bi_1 = Bi_2 = 0.1$ and other parameters listed in Table 1.

Figure 4. The effect of different time dependencies of the incident radiative flux on the exposed surface temperature for $\gamma = 0.16$, $Bi_1 = Bi_2 = 0.1$ and the other parameters as listed in Table 1.

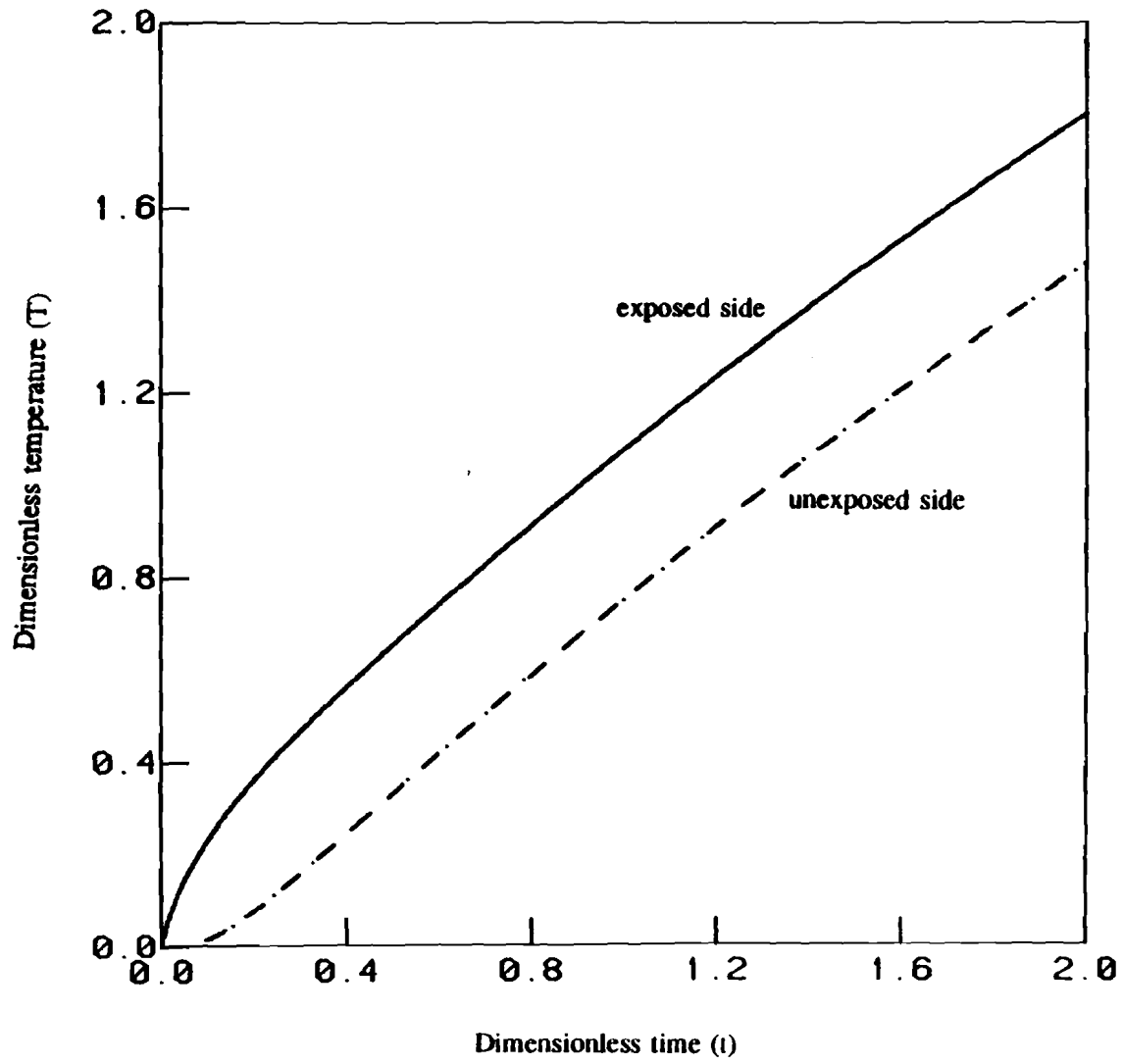


Figure 1.

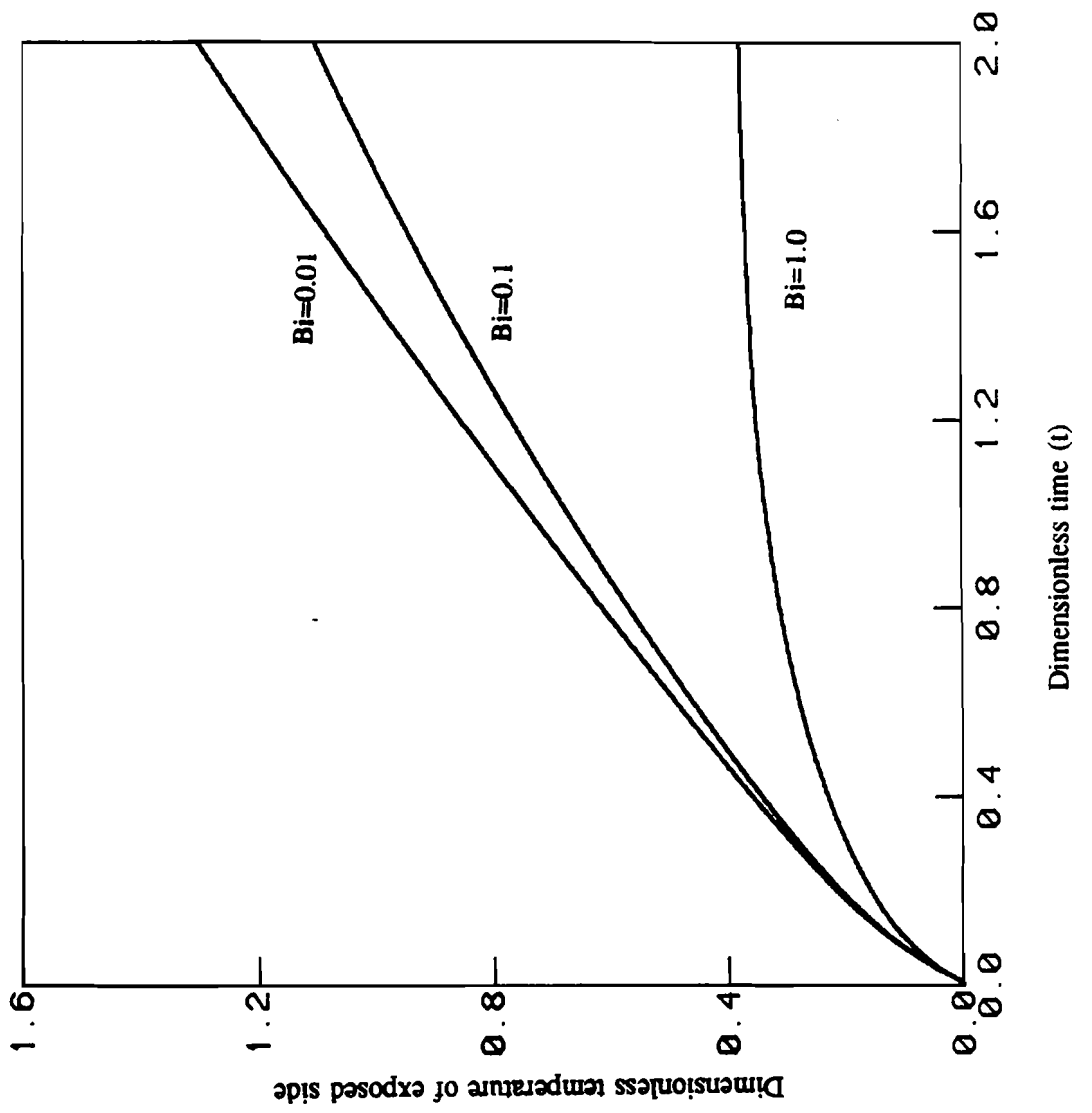


Figure 2a.

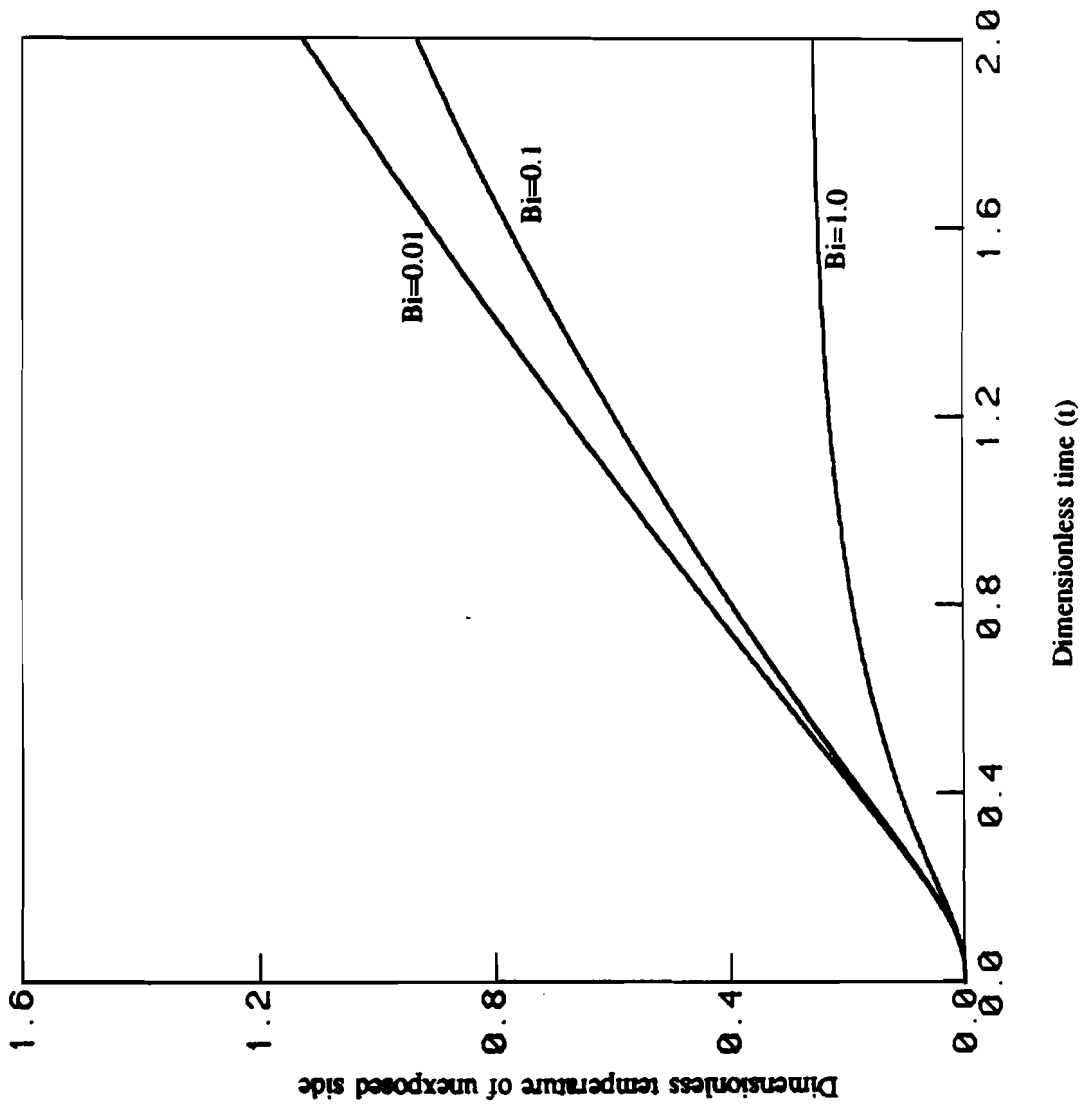


Figure 2b.

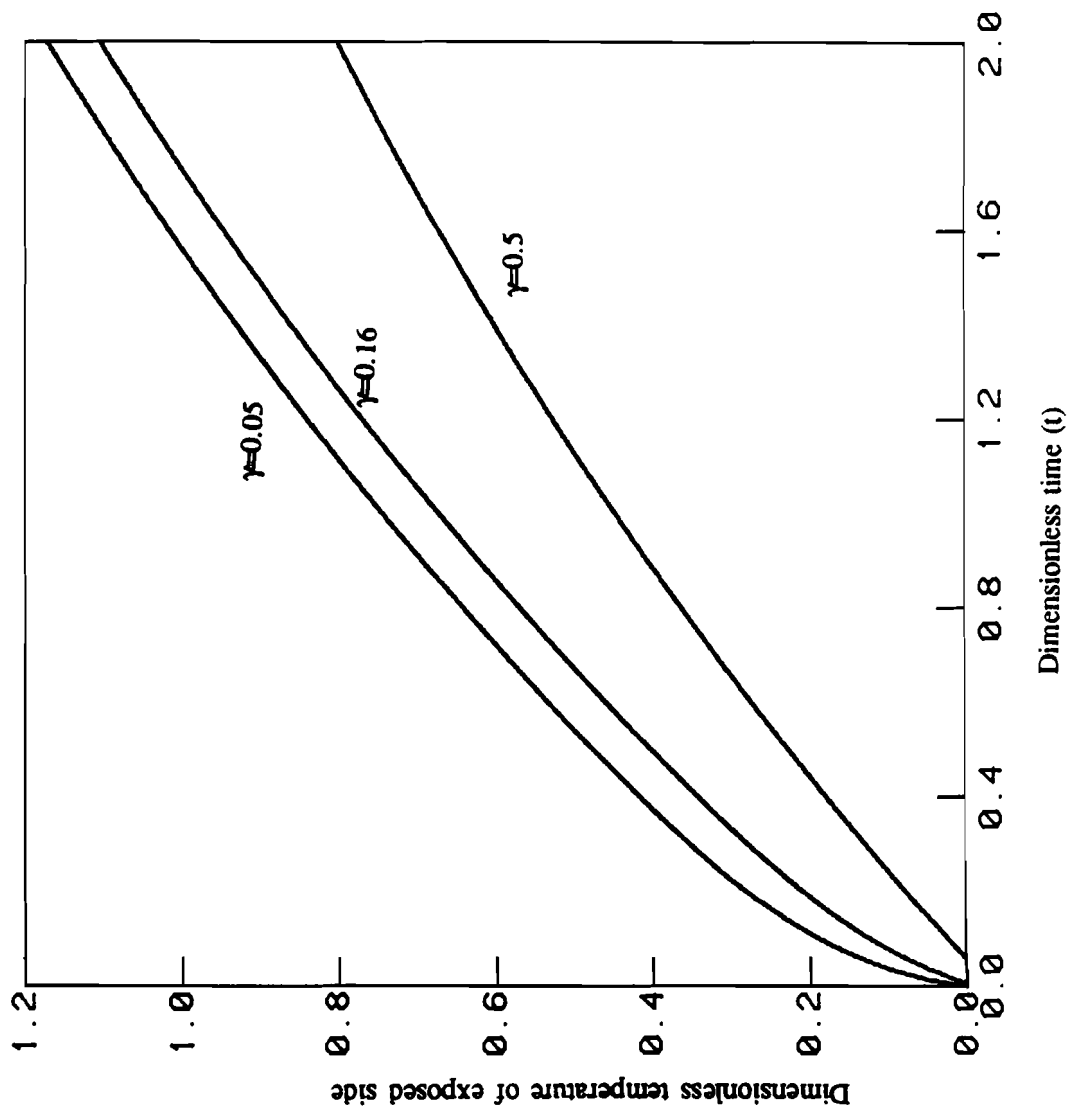


Figure 3.

